20th Australasian Fluid Mechanics Conference
Perth, Australia
5-8 December 2016

PIV Analysis of Coupled Supersonic Twin-Jets

G. Bell[1], J. Soria[1,2], D. Honnery[1], D. Edgington-Mitchell[1]

[1]Department of Mechanical and Aerospace Engineering
Monash University, Victoria 3800, Australia

[2]Department of Aeronautical Engineering
King Abdulaziz University, Jeddah 21589, Kingdom of Saudi Arabia

Abstract

An analysis of the standing-wave present in twin supersonic jets examined and linked to coupling mode. High resolution particle image velocimetry measurements are made for two nozzle pressure ratios, which are selected due to a change in coupling family indicated by a discontinuous jump in screech frequency. A strong nearfield standing-wave is observed for the higher nozzle pressure ratio case where a mismatch between the acoustic screech wavelength and standing-wavelength is observed. A very weak standing-wave is observed in the lower pressure case, which more closely matches the screech wavelength. Two-point velocity correlations reveal a symmetric mode coupling for the higher pressure case. The lower pressure case provided little evidence for plume coupling belonging to an in-plane family oscillation.

Introduction

The twin-jet arrangement is common to many high speed air and spacecraft propulsion systems. The twin-jet configuration can produce intense acoustic radiation. This acoustic radiation has led to fatigue damage to the nozzle structure and empennage in some high speed aircraft, including the F-15 [7]. One major source of acoustic radiation is a self-reinforcing aeroacoustic feedback process called jet screech. Screech occurs in shock containing supersonic jets, as a result of interaction between coherent vortical structures produced at the nozzle lip and downstream shock cells. This shock-vortex interaction produces intense acoustic waves that propagate primarily in the upstream direction. The arrival of these waves at the nozzle lip perturbs the shear layer, producing new coherent vortical structures. Screech has been observed in many single nozzle configurations. It has also been observed in twin and multi jet-configurations, where it is often significantly stronger than the superposition of two single jets would imply. The interaction between downstream convecting coherent structures and upstream propagating acoustic waves forms a standing-wave pattern in the near-field pressure. This standing-wave was identified and quantified through acoustic measurements [5]. The wavelength of the standing-wave has been proposed as a characteristic length-scale for screech. Historically, the shock cell spacing has also been used as a characteristic length scale. Recent work has suggested that a match or mismatch between these length scales is linked to different acoustic feedback mechanism [2]. Despite its importance, the standing-wave has only been experimentally studied using visualization techniques and acoustic measurements.

In a twin jet configuration, the screech cycle is modified by the presence of the adjacent jet, causing the jet plumes to become coupled. The coupling behaviour is a complex function of nozzle spacing and pressure, and can take the form of 4 known modal families of oscillation [4]. The role of the standing-wave in twin-jet coupling has received little attention. Studies of the standing-wave have been primarily limited to more qualitative techniques [6]. While these qualitative measurements of supersonic twin-jets have provided some insight, the limitations of the measurement techniques has precluded fundamental understanding. Very few quantitative flow field studies have been attempted. Notable exceptions include the particle image velocimetry (PIV) study of Alkislar et al. [1].

The objective of this paper is thus to provide a more quantitative experimental study of twin-jet coupling. High-resolution PIV measurements for two modal configurations of coupling are presented. The effect of the standing-wave on the velocity field is determined, and its link to coupling mode examined.

Experimental Setup

The PIV experiments were conducted in the Laboratory for Turbulence Research in Aerospace and Combustion (LTRAC) Supersonic Jet Facility at Monash University. Compressed air at approximately 288 K is supplied directly to a mixing chamber where the free stream and jet are uniformly seeded with smoke particles from a Viscount 1300 smoke generator. The mixing chamber is connected to the plenum chamber, which contains a honeycomb section and wire mesh screens to condition the flow. Compressed air exits twin converging circular nozzles with diameter $D = 10$ mm and nozzle lip thickness of 5 mm. The issued flow is sonic ($M_e = 1$) at the nozzle exit, with a jet exit velocity of $U_e \approx 310\text{m/s}$. A complete overview has been presented in previous work [9].

From previous qualitative studies on the same twin-jet nozzles it was found that an inter-nozzle spacing of 3 ($s/D = 3$) produced strong coupling. Acoustic measurement and analysis were performed to characterise the screech tone of the jet in the PIV facility. The abrupt change in screech frequency at NPR $= 4.85$ in figure **??** was assumed to indicate a transition between an anti-symmetric and symmetric coupling mode in the lateral (co-planar to the jet plane) plane only. This is consistent with the acoustic measurements and phase-locked analysis of Raman [6].

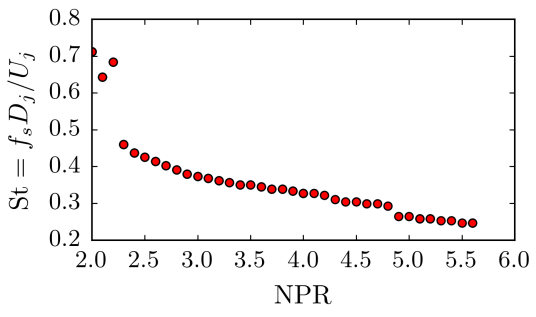

Figure 1: Dominant screech tone for NPR sweep.

Two nozzle pressure ratio (NPR) cases were selected to capture the flow fields of two separate modes detected by the discontinous jump in screech tone of the single microphone acoustic analysis. NPR is commonly expressed as (NPR $= p_0/p_\infty$), which represents the ratio of nozzle stagnation pressure to ambient pressure. Flow features not only in the core jet dynamics but also in the velocity of the surrounding entrainment and acoustic fields were of interest. A dynamic range analysis was performed to ensure flow features involving both large and small particle displacements were adequately resolved. Single exposure image pairs were acquired using a 12-bit Imperx B6640 camera with a CCD array of 6600×4400 px. Approximately 9,000 velocity fields are used for the calculation of all statistics. A spatial of resolution of 19.9×10^{-6} m/px for the centred cases and 19.1×10^{-6} m/px were achieved using a 200 mm Nikon Micro-Nikkor lens. The particle field was illuminated using a diverging light sheet of approximately 1 mm thickness produced from a dual cavity pulsed Nd:YAG laser at 532 nm, with a maximum pulse energy of 200 mJ. A multigrid cross-correlation digital particle image velocimetry algorithm [8] was used to analyse the image pairs. The resulting vector fields have a interrogation window size of 16×16 px with a vector overlap of 50 %, resulting in a vector spacing of 8 px.

Discussion and Results

Mean Flow Fields

A mean flow field of the axial velocity for the NPR $= 5.0$ case is shown in the top half of figure 4a. The lower half shows the NPR $= 4.6$ case. The white regions were masked for the PIV analysis as they contained laser light reflections.

Qualitatively, the flowfields for both cases appear quite similar. Both flows are characterized by a large Mach disk at the first shock cell, and the typical cellular shock-expansion pattern typical of underexpanded jets. In both cases, the jets are quite symmetrical about the internozzle centreline. In neither case are the jets distorted towards each other as observed by Seiner [7]. Quantitatively there are of course some differences. The maximum axial component of velocity is $1.90\,U_j$ for NPR $= 4.6$ and $1.96\,U_j$ for NPR $= 5.0$. The maximum velocities in both cases occur prior to the first shock-cell.

Standard Deviation Fields

The mean velocity field reveals no information pertaining to the standing-wave. However, a signature of the standing-wave is evident in the fluctuating axial velocities for the NPR $= 5.0$ case. The standard deviation of axial velocity for the NPR $= 5.0$ case is presented in figure 4b. A logarithmic scale of the velocity fluctuations has been used to simultaneously resolve the jet core and the smaller fluctuations of the standing-wave structure. The NPR $= 4.6$ contour is excluded for brevity

The standing-wave structure is observed in the NPR $= 5.0$ case as lobes of higher fluctuation in axial velocity. No modulation is apparent in the transverse velocity fluctuations (omitted for brevity). This implies that the motion of the flow and hence the interference between hydrodynamic coherent structures and acoustic waves is predominantly in the axial direction.

Analysis of the Standing Wave

The lobed standing-wave formation is visible both in the internozzle region and on the exterior of the jets. To the authors' knowledge, this is the first time the standing-wave produced by a shock containing supersonic jet has been recorded in the velocity field. The standing-wave was not observed in the studies of Alkislar et al. [1] perhaps due to the limited PIV resolution, and the dynamic-range required to resolve the small motion of the fluid in the entrainment field.

For clarity, figures 2 and 3 present axial profiles of fluctuating axial velocity for the internozzle and jet exterior. These profiles have been detrended to remove the monotonic increase in velocity fluctuations associated with shear layer growth, which dominated the sinusiodal modulation due to the standing-wave. The detrending was accomplished using a 1D Gaussian filter.

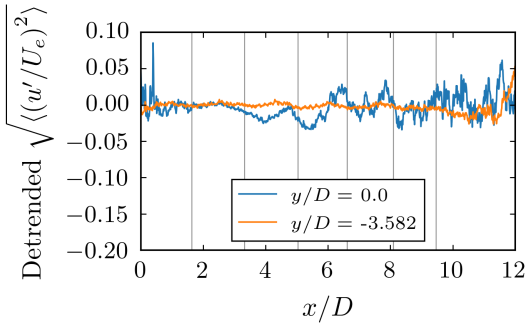

Figure 2: Detrended standard deviation of axial velocity for NPR $= 4.6$. Vertical red lines indicate shock reflection points. No modulation due to a standing-wave is visible.

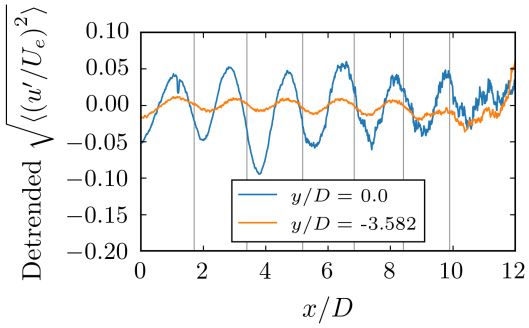

Figure 3: Detrended standard deviation of axial velocity for NPR $= 5.0$. Sinusoidal modulation of the velocity fluctuations indicating a standing-wave structure. Vertical red lines indicate shock reflection points. Further details are provided in table 1.

Figure 2 contains the detrended line plots for the $NPR = 4.6$ case. There is a weak sinusoidal modulation of the axial fluctuations in the internozzle region. No modulation is evident on the jet exterior. Figure 3, for the higher pressure ratio, shows a consistent sinusoidal modulation for both the internozzle and jet exterior profiles.

The discrepancy between the standing-wave for the two cases may be linked to three-dimensionality in the coupling of the plumes. Schlieren path integrated density fluctuations performed by Edgington-Mitchell et al. [2] showed no standing-wave for the out-of-plane flapping modes in an underexpanded elliptical jet. This may provide an explanation for the weak or non-existent standing-wave for the $NPR = 4.6$ case. The standing-wave wavelength and shock spacing are provided in table 1.

Within the two cases examined by Panda [5], he found that the standing-wavelength was less than the shock-cell spacing in both cases. Conversely, Edgington-Mitchell et al. [2] found a standing-wavelength that was greater or equal to the shock-cell spacing for all cases considered. Edgington-Mitchell et

al. [2] reason that this produces a change in upstream propagation mechanism from an external acoustic mode to a shear-layer driven wave-guide model. In the case where the standing-wave is present in this work, the standing-wavelength was found to be greater than the shock-cell spacing. It is unknown whether a predominantly out-of-plane standing-wave exists for the NPR = 4.6 case, which cannot be resolved with an in-plane planar measurement.

Table 1: Screech metrics

	NPR 4.6	NPR 5.0
Screech Strouhl number	0.299	0.264
Screech wavelength, λ_s, ($a = 340$ m/s)	$3.34\,D$	$3.78\,D$
Average shock-cell spacing (first 4)	$1.61\,D$	$1.68\,D$
Average standing-wave spacing, L_{sw}	$\sim 1.56D$	$1.76\,D$

In the 5.0 case, the modulation by the standing-wave is much stronger in the internozzle region. The strength of the standing-wave will be linked to both the amplitude of the upstream propagating acoustic waves and the downstream convecting hydrodynamic waves. Seiner [7] demonstrated that for symmetric coupling mode the overall sound pressure levels in the internozzle region were greater than the sum of two non-interacting single jets. Morris [3] predicted that the increased pressure fluctuations caused by passing coherent hydrodynamic structures drops off exponentially with increasing distance from the shear layer. It is suggested in the present work that the amplitude discrepancy derives from two factors. Firstly, the difficulty of defining a consistent measurement location between the inner and outer jet edges may hinder direct comparison. Secondly, the stronger acoustic field present in the internozzle region should result in a stronger standing-wave [7].

A strong local minima in fluctuating magnitude is visible at an axial location of $x/D \approx 4$ within the internozzle region This was determined not to be an artifact from the Gaussian filter subtraction. Low fluctuation indicates a nodal position in the standing-wave. The root-mean-square acoustic results of Panda [5] show a stronger crest at the 3$^{\text{rd}}$ standing-wave. Further analysis of the acoustic wave propagation and subsequent interference is required to explain this behaviour.

Two-point correlations

The two cases exhibit clear differences in the standing-wave wavelength and amplitude. A possible explanation for this disparity may be a difference in azimuthal instability mode. To assess the spatial structure of the azimuthal instability, two-point correlations were performed on the transverse velocity component and are shown in figures 4c and 4d. The NPR = 5.0 case of figure 4d shows a clear anti-symmetric pattern of opposite correlation function in the jet nearfield field. This is indicative of a symmetric coupling mode about the twin-jet centreline, corresponding to family I as identified by Morris [4]. The NPR = 4.6 case in contrast shows no large scale coherence. Acoustic spectra (not presented here) show comparative screech tone amplitude for the two cases. This similarity in tone strength suggests both flows should be dominated by coherent large scale structures. The lack of coherence evident for NPR = 4.6 suggests that the coupled mode shape for the NPR = 4.6 case is out-of-plane and belongs to either family III or IV.

This difference in coupling behaviour between the two modes also offers an explanation for the disparity in standing-wave amplitude. The symmetric coupling and coherent motion of the NPR = 5.0 case will produce a strong in-plane standing-wave. The symmetry of the coupling explains the higher amplitude of the standing-wave in the internozzle region. Conversely, the lack of in-plane coupling and coherent motion in the NPR = 4.6 case may explain the very weak in-plane standing-wave.

Conclusions

PIV measurements and a subsequent analysis of the standing-wave coupling modality of coupled underexpanded twin-jets has been presented. Two cases have been recorded that are separated by a discontinuous jump in screech frequency. The screech frequency jump is thought to be the result of a change in screech feedback mechanism, accompanied by a change in coupling mode. A strong standing-wave is evident in the velocity fluctuations for the NPR = 5.0 but is much weaker in the NPR = 4.6 case. Analysis by two-point correlation of the velocity fluctuations indicated that the NPR = 5.0 is characterized by a symmetric coupling mode, identified to be family I using the convention of Morris [4]. The symmetric coupling mode allows for the superposition of simultaneously emitted acoustic waves and explains the larger standing-wave amplitude in the internozzle region. The NPR = 4.6 case shows only a weak standing-wave and no in-plane coupling. It is likely to be an out-of-plane coupling mode belonging to family III or IV.

References

[1] Alkislar, M. B., Krothapalli, A., Choutapalli, I. and Lourenco, L., Structure of Supersonic Twin Jets, *AIAA journal*, **43**, 2005, 2309–2318.

[2] Edgington-Mitchell, D., Honnery, D. and Soria, J., Staging behaviour in screeching elliptical jets, *International Journal of Aeroacoustics*, **14**, 2015, 1005–1024.

[3] Morris, P. J., Flow Characteristics of the Large Scale Wave-Like Structure of a Supersonic Round Jet, *Journal of Sound and Vibration*, **53**, 1977, 223–244.

[4] Morris, P. J., Instability waves in twin supersonic jets, *Journal of Fluid Mechanics*, **220**, 1990, 293.

[5] Panda, J., An experimental investigation of screech noise generation, *Journal of Fluid Mechanics*, **378**, 1999, S0022112098003383.

[6] Raman, G. and Taghavi, R., Coupling of twin rectangular supersonic jets, *Journal of Fluid Mechanics*, **354**, 1998, 123–146.

[7] Seiner, J. M., Manning, J. C. and Ponton, M. K., Dynamic Pressure Loads Associated with Twin Supersonic Plume Resonance, *AIAA Journal*, **26**, 1988, 954–960.

[8] Soria, J., An investigation of the near wake of a circular cylinder using a video-based digital cross-correlation particle image velocimetry technique, *Experimental Thermal and Fluid Science*, **12**, 1996, 221–233.

[9] Weightman, J. L., Amili, O., Honnery, D., Soria, J. and Edgington-Mitchell, D., Supersonic Jet Impingement on a Cylindrical Surface, in *22nd AIAA/CEAS Aeroacoustics Conference*, 2016, 2016–2800, 2016–2800.

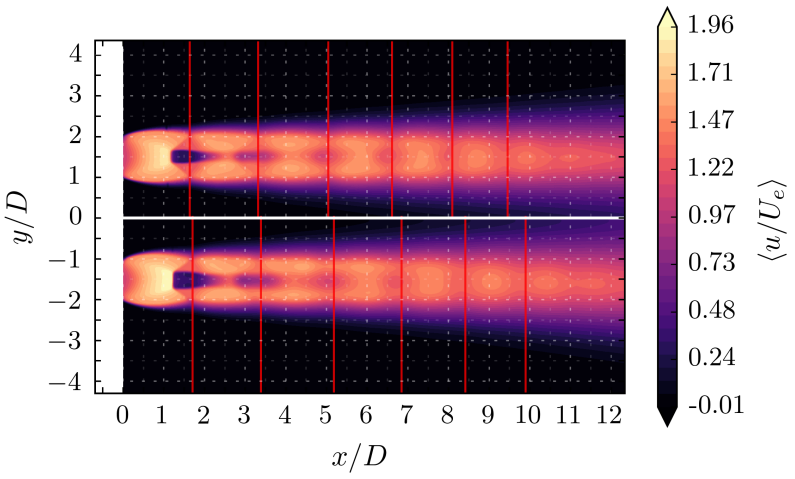

(a) Mean axial velocity. Lower half: NPR = 4.6 Upper half: NPR = 5.0.

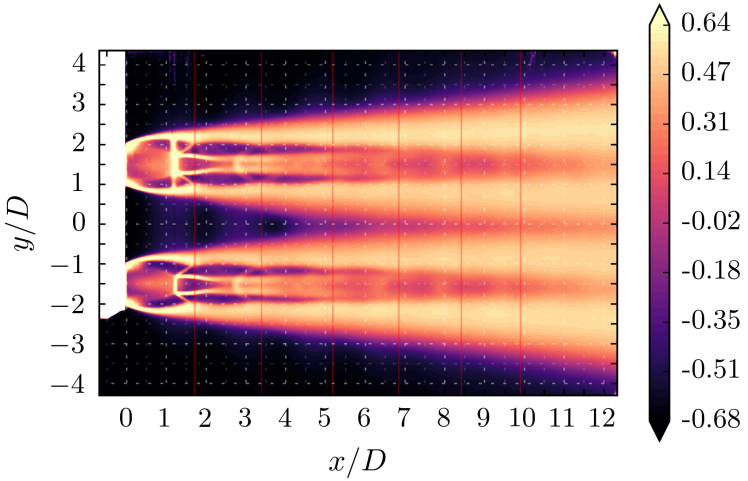

(b) Standard deviation of axial velocity, $\mathrm{Std}(u/U_e) = \log_{10}\left[\sqrt{\langle\langle(u'/U_e)^2\rangle\rangle}\right]$. $\log_{10}$ scale used to increase standing-wave contrast. NPR = 5.0.

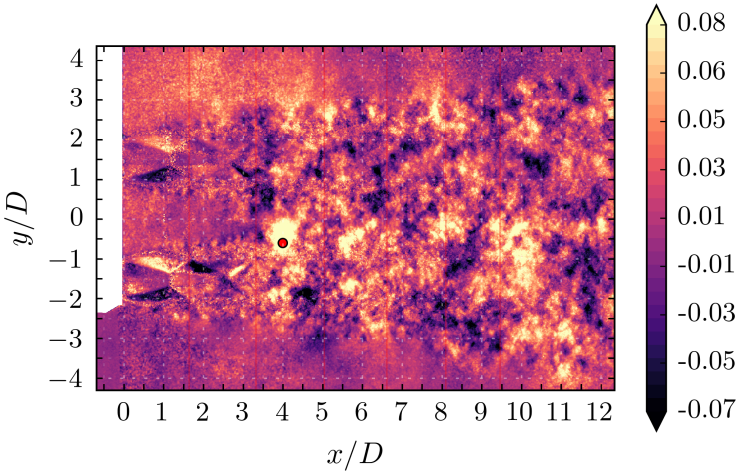

(c) Spearman two point correlation of transverse velocity, $\langle v_1' v_2'\rangle / \sqrt{\langle\langle(v_1')^2\rangle\langle(v_2')^2\rangle}$. Red dot shows reference point. NPR = 4.6.

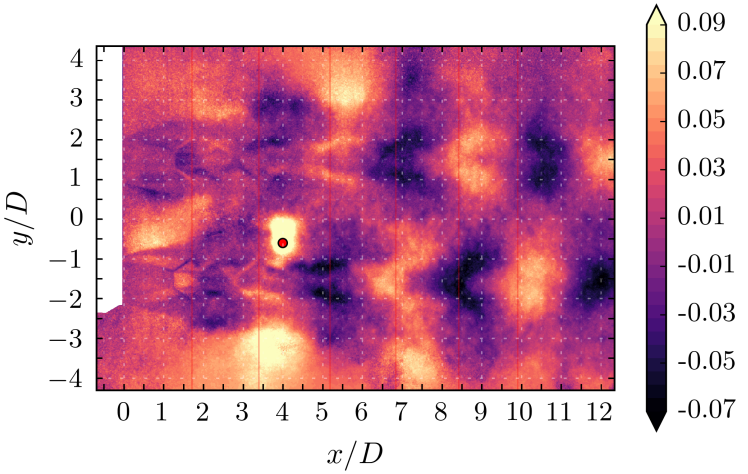

(d) Spearman two point correlation of transverse velocity, $\langle v_1' v_2'\rangle / \sqrt{\langle\langle(v_1')^2\rangle\langle(v_2')^2\rangle}$. Red dot shows reference point. NPR = 5.0.

Figure 4: Contour plots of temporal ensemble statistics.